

Validation of machine learning based scenario generators

Gero Junike*, Solveig Flaig†, Ralf Werner‡

December 12, 2024

Abstract

Machine learning (ML) methods are becoming increasingly important in the design economic scenario generators for internal models. Validation of data-driven models differs from classical theory-based models. We discuss two novel aspects of such a validation: first, checking dependencies between risk factors and second, detecting unwanted memorization effects. The first task becomes necessary since in ML-based methods dependencies are no longer derived from a financial-mathematical theory but are driven by data. The need for the latter task arises since it cannot be ruled out that ML-based models merely reproduce the empirical data rather than generating new scenarios. To address the first issue, we propose to use an existing test from the literature. For the second issue, we introduce and discuss a novel memorization ratio. Numerical experiments based on real market data are included and an autoencoder-based scenario generator is validated with these two methods.

Keywords Nearest neighbor distance, economic scenario generator, memorization ratio, Solvency 2, machine learning

JEL classification C14, C45, C63, G22

*Corresponding author. Institut für Mathematik, Carl von Ossietzky Universität, 26129 Oldenburg, Germany, ORCID: 0000-0001-8686-2661, E-mail: gero.junike@uol.de

†Deutsche Rückversicherung AG, Kapitalanlage-Controlling, Hansaallee 177, 40549 Düsseldorf, Germany, E-Mail: solveig.flaig@deutscherueck.de

‡Institut für Mathematik, Universität Augsburg, 86159 Augsburg, Germany, ORCID: 0000-0001-8204-3757, E-mail: ralf.werner@math.uni-augsburg.de

1 Introduction

Under Solvency 2, insurance companies are required to calculate a Solvency Capital Requirement, i.e., the value-at-risk at the 99.5% level of their own funds over a one-year horizon. This is usually done by generating suitable scenarios using an economic scenario generator and taking the empirical 99.5%-percentile of the loss. This paper focuses on the validation of such machine-learning based economic scenario generators.

Studies that have looked at deriving a value-at-risk based on financial data using neural networks, e.g., generative adversarial networks (GAN), include Tobjörk (2021), Fiechtner (2019) and Flaig and Junike (2022). Arian et al. (2022) and Buch et al. (2023) use (variational) autoencoders to estimate the value-at-risk. Kondratyev and Schwarz (2019) propose a restricted Boltzmann machine for scenario generation. Regulators in several countries, too, have authored papers that address considerations associated with the use of ML methods in internal models. For example, in 2019, the Nederlandsche Bank issued a paper discussing how artificial intelligence is currently used in finance; see van der Burgt (2019). There, the authors state that future ML applications will “use broader and better data to develop predictive risk models” and will “increase the precision of risk assessment”, see van der Burgt (2019, p. 28 and 29). The German regulators, Bundesbank and BaFin, assert that “the use of ML methods can help to quantify risks more accurately and enhance process quality, thereby improving financial firms’ risk management”; nonetheless, these authors also note that “the limited transparency of the model’s behavior has consequences for the [...] model validation”, see BaFin (2021, p. 3 and p. 7). Regulators in other countries, including France (see Dupont et al. (2020)) and the United Kingdom (see Jung et al. (2019)) have also issued papers on this topic.

One of the key processes for internal models in insurance companies is validation, see European Union (2009, Art. 124). BaFin (2021, p. 11), for example, notes that “supervisors are focusing on any new or much more pronounced risks that arise from ML methods.” Therefore, it is important to determine what additional validation measures need to be undertaken in order to prove the validity of a given model when the scenario generator is ML-based.

Basically, in classical internal market risk models, the dependencies between the risk factors (interest rates, equities, foreign exchange) are modeled using financial mathematical tools such as correlations or copulas, see Sandström (2016) or Pfeifer and Ragulina (2018).

In studies that have examined the use of ML methods to generate financial scenarios, validation is carried out primarily by visual means or using only a few statistical parameters, as is the case in Wiese et al. (2019), Ni et al. (2020) and Wiese et al. (2020). In a more quantitative way, Cont et al. (2022) propose an evaluation approach that focuses on the tail of the marginal distributions.

With ML-based models at least two new important issues have arisen which have to be addressed during the model validation process:

i) Since in ML-based models the dependencies are not explicitly modeled, an additional validation has to be performed to show that the dependencies (or, more generally, the multivariate distribution) generated by the model resemble the empirical multivariate distribution including the empirical dependencies.

ii) Another issue associated with generative ML models is the so-called *memorization effect*, see for instance Nagarajan et al. (2018). In this phenomenon, instead of generating new scenarios for risk management purposes, the internal model simply replicates the empirical data used in the learning process. It is well known that neural networks can memorize some training data, see Wei et al. (2024) and references therein. Arora et al. (2018), for example, state that one of the most obvious pitfalls associated with a GAN training is that a GAN may simply memorize the training data. A similar statement holds true for autoencoders as well, see (Radhakrishnan et al., 2018). GANs and autoencoders usually consist of two (potentially coupled) neural networks and both types have already been applied as economic scenario generators in the literature (see above).

The literature on estimating the memorization effect in generative methods focuses mainly on large language models, see Wei et al. (2024) and image generation, see Borji (2019) and Borji (2022) for survey papers. In particular, Lopez-Paz and Oquab (2016) and Xu et al. (2018) propose a 1-nearest neighbor classifier to measure memorization. Bai et al. (2021) propose a memorization-informed Fréchet

inception distance with memorization penalty to evaluate GANs based on cosine similarity. However, the proposed measures of the memorization effect are mainly heuristically motivated metrics which focus on image generation without analyzing the behavior as the sample size of the data increases. Meehan et al. (2020) and van den Burg and Williams (2021) propose a probabilistic approach to measure memorization. However, it requires some data to be withheld for validation, which means that the amount of training data is reduced. This is particularly unfavorable in applications where the training data is sparse.

In the following, we suggest two approaches how to deal with issues i) and ii): To address point i), we propose to use a test based on nearest neighbor distances, as studied by Weiss (1960); Bickel and Breiman (1983); Schilling (1986); Henze (1988); Mondal et al. (2015) and Ebner et al. (2018), which cover both dependencies and marginal distributions at the same time. To address point ii), we develop a new measure called *memorization ratio* to capture the memorization effect. We classify an empirical data point as memorized if a generated data point lies in an unusually small neighborhood around that empirical data point. Our memorization ratio is easy to implement and to interpret. We show that the memorization ratio converges to a dimension-independent constant when the amount of data increases.

We test both measures on simulated and real market data. In particular, our experiments include a real-world example: we use an autoencoder to generate new interest rate scenarios in a high-dimensional space. The training data consists of a term structure interest rate time series from 2000 to 2022. The autoencoder is validated using a nearest neighbor test and our new memorization ratio, demonstrating that the memorization ratio is indeed effective. We further provide in-sample and out-of-sample validation for our data sets.

In particular, out-of-sample validation is a common technique in machine learning to estimate the generalization error, see for instance Goodfellow et al. (2016, Sec. 8), or Gu et al. (2021) who apply out-of-sample validation for autoencoders in a financial context.

The remaining paper is structured as follows: In Section 2, we provide a short background on risk calculation and validation under Solvency 2. In Section 3 we give a brief introduction to neural networks and autoencoders. In Section 4, we introduce the two proposed validation techniques and in Section 5, we show how these techniques can be used for model validation. We consider a one-dimensional real market data set (S&P 500) for illustrative purposes. We also work with multidimensional, autocorrelated simulated data and consider an autoencoder trained on real market data to generate a high-dimensional interest rate term structure. Section 6 concludes.

2 Background: Risk calculation and model validation under Solvency 2

Solvency 2 allows insurers to calculate their risk, which must be backed by capital, in two different ways. Either the standard model is used for this purpose or the insurer develops its own internal model. While in the standard model the method and the weighting factors for all risks are fixed, in the second case the insurer is free to choose the methods, which are quite often based on economic scenarios. More details on the standard model are for example given in European Union (2009, Article 112) or Sandström (2016, Appendix I). For a critical review of the standard model let us refer to Scherer and Stahl (2021). An introduction to economic scenario generators is for instance provided by Pedersen et al. (2016). See Bégin (2021) for Monte Carlo simulations for internal models. Varnell (2011) provides a non-technical view on economic scenario generation under Solvency 2. A comparison of the standard model and internal models for calculating Solvency 2 capital requirements is carried out in Shedari (2016) or Gatzert and Martin (2012).

Often, a historical simulation is implemented in order to estimate a (short horizon) value-at-risk, see Hendricks (1996) and Beder (1995) for an analysis of the empirical performance of such simulation. In a historical simulation, similar to bootstrapping, empirical data is simply copied to “generate” future scenarios. Similarly, Demirel and Willemain (2002), Müller et al. (2004) and Albeanu et al. (2008) propose a bootstrap method for scenario generation. A critical view on the topic is for example due to Pritsker (2006). Quite related, Adesi (2014) propose a filtered historical simulation approach, where historical returns are multiplied by the ratio of the historical volatility and the current volatility.

To ensure comparability of risk calculations, insurers determining their risk using an internal model must meet certain requirements. A very important one relates to the regular validation of the internal model. According to European Union (2009, Art. 124), this “includes monitoring the performance of the internal model, reviewing the ongoing appropriateness of its specification, and testing its results against experience”.

Current internal models for market and non-life underwriting risk often use Monte-Carlo simulation techniques to derive the risk of the (sub)modules and then use correlations or copulas for aggregation, see Pfeifer and Ragulina (2018). On the market risk side, the risk calculation is often based on an economic scenario generator (ESG); this approach produces realistic scenarios how the risk factors may evolve over a certain time horizon, which is set to one year in Solvency 2, see Cadoni (2014, p. 190). Traditional ESG approaches implement financial-mathematical models for all relevant risk factors (e.g. interest rate, equity) and their dependencies. Under these scenarios, the asset and liability portfolio of the insurer is evaluated and the risk is given by the 99.5%-percentile of the loss in these scenarios. The models for non-life underwriting risk also simulate scenarios as to how the claims evolve and these scenarios are then used to derive the risk, see Cadoni (2014, p. 192).

However, it is not appropriate to limit the validation of ML-based models to the methods used for classical financial-mathematical models. In this context, the German regulator, BaFin, warns that “Supervisory practice for ML methods can [...] be derived from the existing framework. At the same time, an outlier analysis, also supported by this consultation, is currently surveying the areas in which the supervisory inspection approach needs to be fleshed out in order to cater to the peculiarities of using ML methods.”, see BaFin (2021, p. 11). This means that the validation for an internal model can basically remain the same, but any special features of the ML-based approach must additionally be taken into account and validated.

3 Background: Neural networks and autoencoders

A *neural network* is a system that is broadly inspired from the human brain. It can transform a (one- or more-dimensional) input into a (one- or more-dimensional) output. A neural network consists of *neurons* which are arranged in *layers*. The neurons of one layer are connected to the neurons of the next layer. All starts with the *input layer*, which is then followed by one or more so called *hidden layers* and ends with the *output layer*, as Figure 1 based on Fernandez-Arjona (2021, Fig. 1) illustrates. A detailed and more thorough treatment of neural networks can be found in Goodfellow et al. (2016).

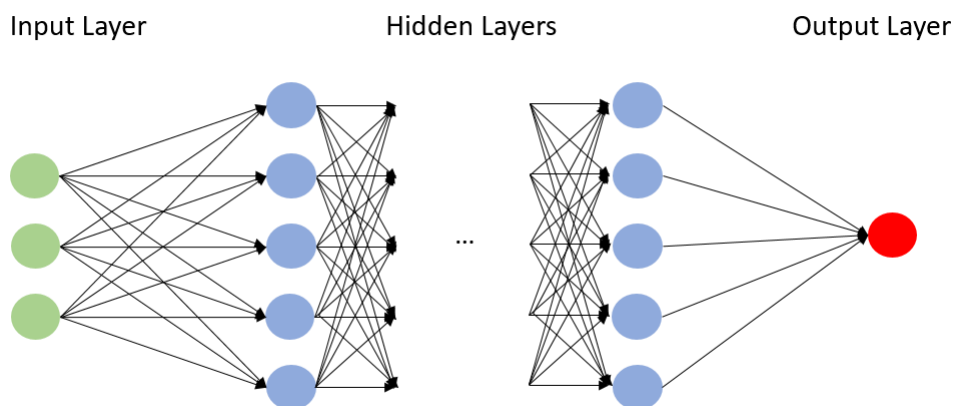


Figure 1: Neural network structure, based on Fernandez-Arjona (2021, Fig. 1).

All neurons transform their multi-dimensional input (which comes from either the input layer or the preceding hidden layer) via a so called *activation function* into an one-dimensional output which is then transferred to all the neurons in the next layer.

A typical choice for an activation function g is the rectified linear unit $g(t) = \max(t, 0)$. For a

neuron input $x \in \mathbb{R}^n$ and *parameters* or *weights* $w \in \mathbb{R}^{n+1}$ the output of the neuron is then given by $g(\sum_{i=1}^n w_i x_i + w_{n+1})$.

The parameters in the activation function in each neuron are often initialized randomly. Afterwards, these parameters are optimized when giving the neural network training data consisting of pairs of input data and the desired output so that the output of the neural network resembles the desired output given the training data.

In the numerical section, we will use a special type of neural network, an autoencoder, in a generative fashion as an economic scenario generator. For this purpose, let us briefly explain the main functionality of an autoencoder. An *autoencoder* consists of two neural networks: an *encoder* network $\mathcal{E}_\phi : \mathbb{R}^d \rightarrow \mathbb{R}^k$ with parameters ϕ and a *decoder* network $\mathcal{D}_\theta : \mathbb{R}^k \rightarrow \mathbb{R}^d$ with parameters θ . Autoencoders can be employed for a variety of tasks; most prominently, autoencoders can be used for dimension reduction, where $d \gg k$ holds. In such a setup, autoencoders can be interpreted as a nonlinear version of the traditional principal component analysis. For more details on autoencoders as well as on further applications, let us refer to Goodfellow et al. (2016).

Concerning the training of autoencoders, let E be a d -dimensional random variable and let E_1, \dots, E_M be M independent copies of E . Since the decoding and encoding is not perfect, a reconstruction error $E_m - \mathcal{D}_\theta(\mathcal{E}_\phi(E_m))$ on the m -th input E_m cannot be avoided. Training is usually achieved by minimization of these reconstruction errors by an appropriate reconstruction loss function (like the following mean-square loss L , or more generally some p -norm) via some (stochastic) gradient descent method:

$$L(\phi, \theta) := \frac{1}{M} \sum_{m=1}^M \|E_m - Y_m\|_2^2 \longrightarrow \min! \quad \text{with } Y_m := \mathcal{D}_\theta(\mathcal{E}_\phi(E_m)).$$

Let us assume that the parameters ϕ and θ of the autoencoder are obtained by some training method and that (in-sample and out-of-sample) reconstruction errors are small enough. Then, the decoder can be used in a generative fashion, if the (low-dimensional) distribution of the so-called *latent factors* $Z := \mathcal{E}_\phi(E)$ is (approximately) known: to generate N new samples for E , let Z_1, \dots, Z_N be independent copies of Z and set

$$G_n := \mathcal{D}_\theta(Z_n), \quad n = 1, \dots, N.$$

In our selected example in Section 5.3, we will see that although Z might not be multivariate normal distributed, it can still be approximated sufficiently well by such a distribution, which allows to use the autoencoder in a generative manner as an economic scenario generator.

If $Z = \mathcal{E}_\phi(E)$ cannot be easily approximated by some appropriate multivariate distribution, the autoencoder can be enhanced to an *adversarial* or to a *variational autoencoder*. Very briefly speaking, these enhanced setups change the encoder-decoder pair $(\mathcal{E}_\phi, \mathcal{D}_\theta)$ in such a way that $\mathcal{E}_\phi(E)$ is approximately multivariate normal distributed while keeping the encoding-decoding performance, see Kingma and Welling (2019) and Makhzani et al. (2015) for more details.

4 Validation techniques for machine learning based scenario generators

During the usual validation cycle, insurers already investigate a variety of statistical properties of a scenario generator. For example, stability and sensitivities are typically already part of established validation procedures. However, within an ML-based approach, some additional validation is required as we have already pointed out in the introduction: Since the multivariate distribution of the risk factors is not derived from a financial mathematical model, it has to be verified that the generator only produces samples from the same (or at least very similar) distribution as implied by the data sample. Further, since a pure resampling method is not intended by an ML-based generator, it is necessary to analyze for potential memorization effects.

Here, we suggest a purely data-driven non-parametric evaluation approach, because the non-parametric nature is one of the main advantages of using ML-based generators. Such methods which can be applied to any model are generally referred to as *model agnostic*, see e.g., Borji (2019, p. 4). Furthermore, we prefer quantitative measures which are easily interpretable and computationally not

too expensive, thus fostering their use in validation purposes in a Solvency 2 regime. For this purpose, we split the recommended validation techniques into two components:

- (1) the alignment of the multivariate distributions in the given empirical data and in the generated data, and
- (2) the memorization effect.

Measures for these two categories are discussed in the subsequent Subsections 4.1 and 4.2. Like any other test statistics, these kind of methods could be used not only for validation, but also for hyperparameter optimization of the ML models. Of course, additional validation, for example of marginal tail behavior, could be carried out using the quantitative measures based on value-at-risk and expected shortfall as proposed in Cont et al. (2022, p. 21) or by comparison to benchmark portfolios as in Flaig and Junike (2022, Chapter 3).

For the mathematical discussion in the remainder of this paper, we rely on the following notation: Let (Ω, \mathcal{F}, P) be a probability space and $d \in \mathbb{N}$ the number of risk factors that are modeled. Further, let $E : \Omega \rightarrow \mathbb{R}^d$ denote a random vector describing the empirical data. The data generated by some ML-based generator is denoted by the random vector $G : \Omega \rightarrow \mathbb{R}^d$. Finally, let E_1, \dots, E_M , and G_1, \dots, G_N be independent copies of the random vector E and G , respectively. Since the consideration of memorization effects is mainly important for continuous distributions, we make the following main assumption:

Assumption H0. *The random variables $E_1, \dots, E_M, G_1, \dots, G_N$ are independent and identically distributed and have a piecewise continuous and bounded probability density function.*

4.1 Measure for the alignment of the multivariate distributions: Nearest neighbor coincidence

The test on the alignment of the multivariate distribution including dependency and marginal distributions of the empirical and the generated data can be reformulated as a multivariate two-sample test where we want to measure the equality of two multivariate distributions based on two sets of independent observations. For this purpose, and in alignment with the above considerations, we prefer the *nearest neighbor coincidence measure* as defined by Schilling (1986) and as further developed by Mondal et al. (2015). This test statistic is rather easy to interpret and to implement, computationally cheaper than alternative methods (for example, based on optimal transport) and the numerical experiments by Mondal et al. (2015) are very promising. Of course, alternative possibilities for checking equality of distributions are available, e.g., maximum mean discrepancy, average log-likelihood, F1-score, and many more, see for instance Borji (2019).

For the definition of the nearest neighbor coincidence let us consider the indicator function $\delta_{E_m}(r)$ which takes the value 1 if the r -nearest neighbor (measured by the Euclidean distance) of E_m within the set $\{E_1, \dots, E_M, G_1, \dots, G_N\} \setminus \{E_m\}$ is an empirical data point and 0 if it is a generated data point. Accordingly, the indicator function $\delta_{G_n}(r)$ is 1 if the r -nearest neighbor is a generated data point and 0 otherwise. As in Mondal et al. (2015), we define for $k \in \mathbb{N}$:

$$T_{NN1,k} = \frac{M|T_{E,k} - \frac{M-1}{N+M-1}| + N|T_{G,k} - \frac{N-1}{M+N-1}|}{N+M}, \quad (1)$$

where

$$T_{E,k} = \frac{1}{Mk} \sum_{m=1}^M \sum_{r=1}^k \delta_{E_m}(r) \quad \text{and} \quad T_{G,k} = \frac{1}{Nk} \sum_{n=1}^N \sum_{r=1}^k \delta_{G_n}(r).$$

The test statistic $T_{E,k}$ (the test statistic $T_{G,k}$) counts for each empirical (generated) data point the number $r \leq k$ of neighbors which are also empirical (generated) data points and takes the average. Under Assumption H0, $T_{NN1,k}$ should be close to 0. If the empirical data points and the generated data points are rather distinct from each other (i.e. stem from different distributions), $T_{NN1,k}$ should take larger values due to lack of full mixing of the two samples. In particular, for $M = N$ and if the generated data is far off the empirical data, $T_{E,k}$ and $T_{G,k}$ should be both close to their maximum value 1 and $T_{NN1,k}$ should be close to $\frac{1}{2}$.

Remark 1. Mondal et al. (2015) prove that $\sqrt{N+M} \cdot T_{NN1,k}$ is asymptotically distributed as a sum of two correlated half normals if Assumption H0 holds and if N and M grow to infinity with $\frac{M}{N} \rightarrow \alpha$ for some $\alpha > 0$. It is further shown that under Assumption H0, the expectation of $T_{E,k}$ is equal to $\frac{M-1}{N+M-1}$ and the expectation of $T_{G,k}$ is equal to $\frac{N-1}{M+N-1}$.

Remark 2. To compute $T_{NN1,k}$, we have to find the minimum entry of a vector of length $M+N$ exactly M respectively N times, to obtain $T_{E,k}$, resp. $T_{G,k}$. The computational effort for the computation of $T_{NN1,k}$ is therefore at most $O((N+M)^2)$.

An implementation of $T_{NN1,k}$ can be found in Appendix C.

4.2 Measure for the detection of memorization: memorization ratio

The statistic $T_{NN1,k}$ will lead to very good scores if the generated data are drawn with repetition from the empirical ones (bootstrapping). From a risk management perspective, this is not the optimal result because the main intention of employing a generative ML-based generator is to create new scenarios that could happen rather than memorizing scenarios that have actually taken place, see Chen et al. (2018, p. 2). Bai et al. (2021, p. 1) emphasize that “unintentional memorization is a serious and common issue in popular generative models”. Therefore, we need some (preferably interpretable) quantitative measure to detect whether generated data points match empirical ones or not.

In a multi-dimensional space, it is highly unlikely for generated and empirical data points to match exactly, so we classify an empirical data point as being memorized if a generated data point lies in “an unusual small neighborhood” around this empirical data point.

Definition 1. Let $\rho \in (0, 1]$. The *memorization ratio* $\Pi_{M,N}^\rho$ is defined as:

$$\Pi_{M,N}^\rho = \frac{1}{M} \sum_{m=1}^M \mathbf{1}_{[0, \rho^{\frac{1}{d}} R_m)} \left(\min_{n=1, \dots, N} \|G_n - E_m\|_2 \right) \quad (2)$$

where

$$R_m := \min_{m' \neq m} \|E_m - E_{m'}\|_2, \quad m = 1, \dots, M. \quad (3)$$

The random variable R_m denotes the distance between E_m and its nearest empirical neighbor. An Euclidean ball of radius $\rho^{\frac{1}{d}} R_m$ has a volume equal to a fraction ρ of the volume of a ball of radius R_m . An empirical data point E_m is considered *memorized* if there is at least one generated data point inside the ball of radius $\rho^{\frac{1}{d}} R_m$ around E_m , compare with Figure 2. The memorization ratio equals the percentage of elements E_1, \dots, E_M which are memorized. If all empirical data is memorized, then $\Pi_{M,N}^\rho = 1$. If no empirical data is memorized, then $\Pi_{M,N}^\rho = 0$. An implementation of $\Pi_{M,N}^\rho$ can be found in Appendix C.

Remark 3. The parameter ρ allows to control the interpretation of memorization: The smaller ρ , the less likely it is that an empirical data point is deemed memorized. In the extreme case that ρ approaches zero, an empirical data point will only be considered memorized if there is an identical generated data point. This happens, for example, when the empirical data is simply copied, e.g., during bootstrapping. The greater ρ , the more likely it is that an empirical data point is considered memorized. The special case $\rho = 1$ is related to the measure “1-NN accuracy (real)” in Xu et al. (2018, p. 3). Most importantly, our approach is more general and backed by mathematical results: for instance, the subsequent Theorem 1 establishes convergence of the memorization ratio $\Pi_{M,N}^\rho$ to a dimension-independent limit.

Theorem 1. Let $\alpha > 0$ and $\rho \in (0, 1]$. Under Assumption H0, it holds in the mean square sense that

$$\lim_{M, N \rightarrow \infty, \frac{M}{N} = \alpha} \Pi_{M,N}^\rho = \frac{\rho}{\rho + \alpha}.$$

Proof. The proof can be found in Appendix A. □

Remark 4. According to Theorem 2 of Weiss (1960), the limit $\frac{\rho}{\rho + \alpha}$ of the memorization ratio under H0 equals the asymptotic probability that an arbitrarily empirical data point is memorized.

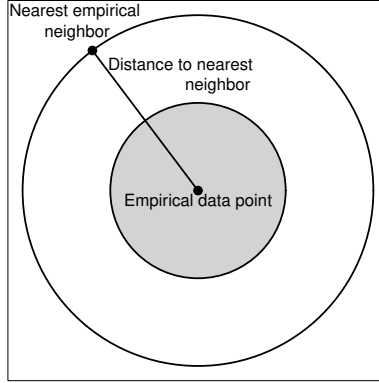


Figure 2: Memorization ratio with $\rho = 0.25$. If there is at least one generated point within the gray area, the empirical data point is considered memorized. The gray area corresponds to 25% of the whole area of the circle.

The convergence of the memorization ratio to its theoretical limit stated in Theorem 1 can also be observed empirically in Table 1 for normal distributed as well as non-normal distributed random variables.

The benefit of the memorization ratio can be visualized in Figure 3. Some empirical data is compared to two different sets of generated data. Both generated data sets are fine according to the statistic $T_{NN1,k}$, i.e., are similarly distributed as the empirical data. However, one generated data set leads to a high memorization ratio and can thus be ruled out.

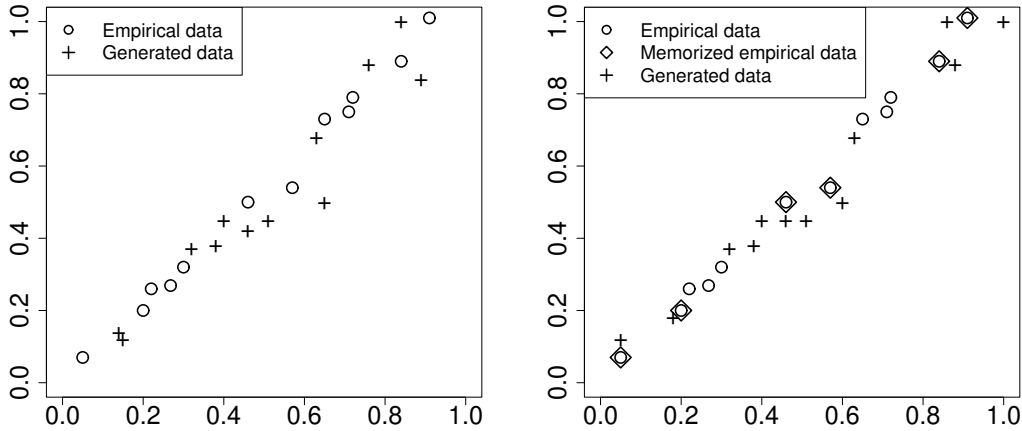


Figure 3: Example for the benefit of the memorization ratio; on the left: $T_{NN1,k} = 0.02$, $\Pi_{M,N}^\rho = 0$; on the right: $T_{NN1,k} = 0.02$, $\Pi_{M,N}^\rho = 0.5$, where $k = 3$ and $\rho = 0.25$.

	ρ	Two corr. Gaussian	Exp. and Cauchy	20 uniform	Theoretical limit
$M = 100, N = 100$	0.25	0.200	0.207	0.275	0.200
$M = 100, N = 400$	0.25	0.496	0.506	0.598	0.500
$M = 200, N = 100$	0.25	0.109	0.114	0.159	0.111
$M = 100, N = 100$	0.5	0.333	0.338	0.392	0.333
$M = 100, N = 400$	0.5	0.661	0.676	0.706	0.667
$M = 200, N = 100$	0.5	0.198	0.205	0.234	0.200

Table 1: Memorization ratio for different distributions: Consider four independent random variables: let X_1, X_2 be standard normal distributed, X_3 exponentially distributed with rate one and X_4 Cauchy distributed with location zero and scale one. Let $E_1, \dots, E_M, G_1, \dots, G_N$ be independent copies of $(X_1, \gamma X_1 + \sqrt{1 - \gamma^2} X_2)$ with correlation $\gamma = 0.75$ for the column “Two corr. Gaussian”. Let them be independent copies of (X_3, X_4) for the column “Exp. and Cauchy”. For the column “20 uniform”, let them be independent copies of 20 independent, uniform distributed random variables. We average the memorization ratio over 100 simulations. Each entry in the table comes with a standard error of at most ± 0.006 . The values in the table hardly change choosing the norm $\|\cdot\|$ for the memorization ratio as defined in Remark 5.

Remark 5. If a generated data point $G = (G^1, \dots, G^d)$ is identical to an empirical data point $E = (E^1, \dots, E^d)$ in all dimensions except, say, the first dimension, it depends on the application whether E should be deemed ‘memorized’ or not. Choosing the Euclidean distance as in Definition 1, we obtain

$$\|G - E\|_2 = |G^1 - E^1|$$

and E would usually *not* be considered as memorized if G^1 and E^1 are different enough. In some applications, this might not be desirable, i.e., E should be deemed memorized since it is almost indistinguishable from G . One solution would be to choose another metric for the memorization ratio, e.g. based on the norm

$$\|x\| := \underbrace{\frac{2}{\sqrt{\pi}} \left(\frac{\Gamma(\frac{d}{2} + 1)}{d!} \right)^{\frac{1}{d}}}_{=: \beta(d)} (|x^1| + \dots + |x^d|), \quad x \in \mathbb{R}^d.$$

A unit ball under $\|\cdot\|$ has the same volume as a unit ball under $\|\cdot\|_2$. Since $\beta(d) \rightarrow 0$ for $d \rightarrow \infty$, we then have

$$\|G - E\| = \beta(d)|G^1 - E^1| \rightarrow 0, \quad d \rightarrow \infty$$

and E is always deemed memorized if d is large enough. This is also confirmed numerically in Table 2.

d	MR with $\ \cdot\ $	MR with $\ \cdot\ _2$
10	0.02	0.0
20	0.98	0.002
30	1.0	0.02

Table 2: Take $M = N = 1000$, E_1, \dots, E_M are independent and multivariate normally distributed in \mathbb{R}^d with mean zero and covariance matrix equal to the identity. We set G_1 independent of E_1, \dots, E_M but with mean equal to $(8, \dots, 8)$ and covariance matrix equal to the identity and $G_i := E_i$, $i = 2, \dots, M$. The memorization ratio (MR) is obtained for $\rho = \frac{1}{2}$ and using the norm $\|\cdot\|$ and $\|\cdot\|_2$. The entries in the table come with a standard error of at most ± 0.0005 .

Remark 6. Motivated by a reviewer’s remark, we comment on a potential generalization of Theorem 1: the convergence result should also hold for identically distributed E_m with a finite range dependence

(i.e. all E_{m+k} are independent of E_m for $k \geq K$); thus allowing for finitely overlapping estimation windows in time series. Figure 6 indicates that such a statement should hold true, but we leave a potentially more technically involved proof for future research.

Remark 7. Denote by P_E the distribution of E and by P_G the distribution of G . By P_E^M and P_G^N we denote the empirical distribution of an empirical sample of size M and a generated sample of size N . Arora et al. (2017) and Cont et al. (2022) define the generalization error of P_G by

$$|d(P_E^M, P_G^N) - d(P_E, P_G)|, \quad (4)$$

where d represents a divergence, e.g., the Wasserstein distance, quantile divergence, the neural net distance, etc., see Arora et al. (2017); Cont et al. (2022) and references therein. A large probability of a small generalization error means that the generator has a similar performance with the empirical distributions and the true distributions, i.e., generalizes well from the training data set. However, this definition does not capture the memorization effect: Assume P_E and P_G are one-dimensional standard normal distributions. Consider some empirical data of size M distributed according to P_E and generate data by simply bootstrapping (draw M times independently with repetition) from the empirical data. If d is the Wasserstein distance, the generalization error of P_G converges to zero in probability for $M \rightarrow \infty$ but the training sample is memorized since bootstrapping does not generate new, unseen samples.

5 Numerical experiments

In this section, consider three different setups: in Section 5.1, we apply the concepts to one-dimensional real market data for illustrating purpose. In Section 5.2, we work with four-dimensional, auto-correlated simulated data. In Section 5.3, we investigate in detail a purely data driven setup and deal with high-dimensional, real-market interest rate data and autoencoders.

5.1 Illustrating one-dimensional example

In this section we illustrate in a simple setting how the memorization ratio and the test statistic $T_{NN1,k}$ can be used to evaluate various approaches to generate new samples from a training set.

We consider a training set consisting of the yearly log-returns of the S&P 500 from 1997 to 2011 and a test set of the years 2012 to 2023. We discuss several ways to generate new samples from the training data, i.e., bootstrapping, a parametric approach and a ML-based method:

- **Bootstrapping:** to generate new samples, we simply draw independently with repetition from the training set (with $N = M$). The probability that a scenario from the training set shows up in the bootstrap-sample, and is hence memorized, is $1 - (1 - \frac{1}{M})^M \approx 1 - e^{-1} = 0.63$, cf. Table 3.
- **Parametric model:** we use the normal distribution with mean and standard deviation equal to the empirical mean and standard deviation of the training data set to generate new samples.
- **Data-driven with kernel-smoothing:** we calibrate a kernel-smoothed cumulative distribution function with Gaussian kernel with global bandwidth $h > 0$ to the training data and use that distribution to generate new samples, i.e., we use the CDF

$$F_h(x) = \frac{1}{M} \sum_{m=1}^M \Phi\left(\frac{x - E_m}{h}\right), \quad x \in \mathbb{R},$$

where Φ is the CDF of a standard normal random variable and E_1, \dots, E_M is the training data.

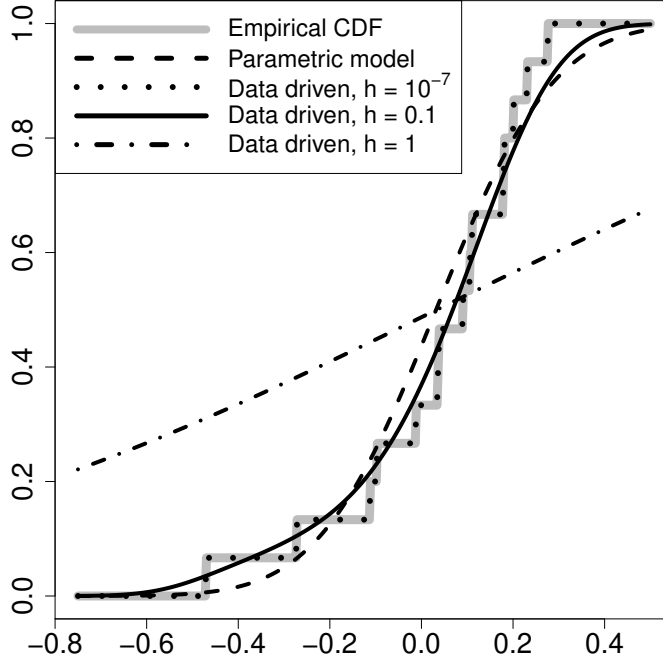


Figure 4: Several CDFs to generate new data.

The empirical CDF of the training set and the CDFs of the various data generation methods are shown in Figure 4. In Table 3, we provide the test statistic $T_{NN1,k}$ and the memorization ratio for the generated data versus the training set (in-sample) and the generated data versus the test set (out-of-sample). We observe that all data generation methods except the one based on kernel-smoothing with $h = 0.1$ and the parametric model show severe deficits: Bootstrapping and kernel-smoothing with a very small h result in a very high memorization ratio: overfitting takes place because the empirical CDF is just memorized. Underfitting occurs when the bandwidth for kernel-smoothing is too large, because the kernel-smoothed CDF does not reproduce the empirical distribution function very well. In general, underfitting can be easily discovered by large values of the test statistic $T_{NN1,k}$. We note that in this very simple setting, the parametric model fits the distribution reasonably well. Unfortunately, especially for larger dimensions, adequate parametric models cannot always be determined. For example, in Section 5.3, we use an autoencoder-based approach to generate yield curves (of dim 31); a setup where most parametric models are known to have some issues, especially in the dependence structure of different maturities.

Data generation Method	$T_{NN1,k}$ in-sample	MR in-sample	$T_{NN1,k}$ out-of-sample	MR out-of-sample
Bootstrap	0.06	0.64	0.08	0.11
Data-driven, $h = 10^{-7}$	0.05	0.65	0.07	0.14
Data-driven, $h = 1$	0.22	0.08	0.27	0.07
Data-driven, $h = 0.1$	0.06	0.19	0.07	0.19
Parametric model	0.06	0.17	0.07	0.21

Table 3: In-sample and out-of-sample validation using the memorization ratio (MR) with $\rho = 0.25$ and the test statistic $T_{NN1,k}$ with $k = 3$. In-sample ($M = N = 15$): empirical data is the training set. Out-of-sample ($M = N = 12$): empirical data is the test set. Unacceptable values are displayed in bold. We average over 100 simulations. Since $M = N$, under H_0 , the memorization ratio converges to $\frac{\rho}{\rho+1} = 0.2$ for in-sample validation and out-of-sample validation. The entries in the table come with a standard error of at most ± 0.01 .

Figure 5 shows the memorization ratio versus the statistic $T_{NN1,k}$, where the empirical data is the training set and new samples are generated by a data-driven approach using kernel-smoothing with different bandwidths $h > 0$, bootstrapping and a Monte Carlo simulation via a parametric model. The optimal scenario generator can be chosen such that the memorization ratio is close to its theoretical limit and the statistic $T_{NN1,k}$ is small.

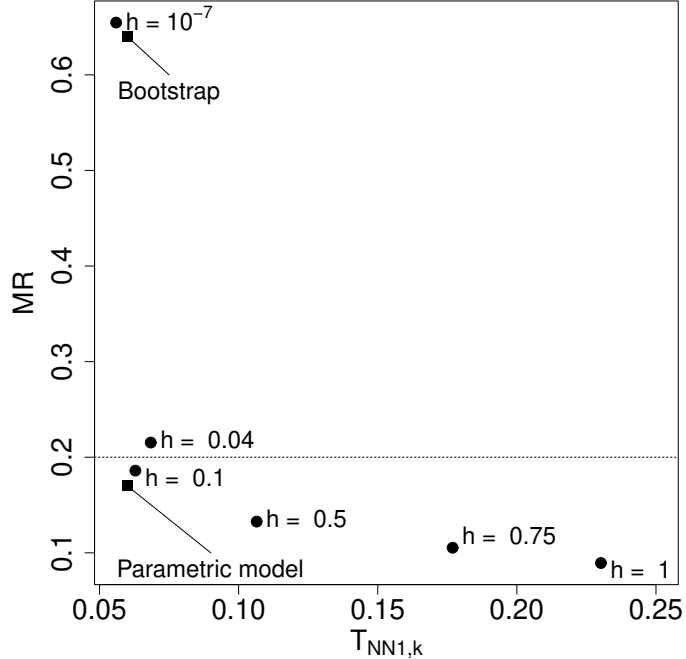


Figure 5: Memorization ratio (MR) with $\rho = 0.25$ versus $T_{NN1,k}$ with $k = 3$. New samples are generated by a data-driven approach using kernel-smoothing with different bandwidths $h > 0$, bootstrapping and a Monte Carlo simulation via a parametric model. Generated scenarios are compared to the training set. The theoretical limit of the memorization ratio is 0.2. We average over 100 simulations.

5.2 Dependent data

For illustration purposes, we simulate four dimensional financial daily data by a (correlated) geometric Brownian motion. Technical details can be found in Appendix B. We apply a rolling (estimation) window to this data in order to construct financial scenarios over a larger time horizon. Let $w \in \mathbb{N}$ be some appropriate window size, e.g., $w = 5$, $w = 21$ and $w = 63$ corresponds to weekly, monthly or quarterly data. If $w > 1$, the data becomes auto-correlated in the time-dimension, due to window overlapping. We see in Figure 6 that the memorization ratio still seems to converge (even though the independence assumption in H_0 is violated) with the same order of convergence.

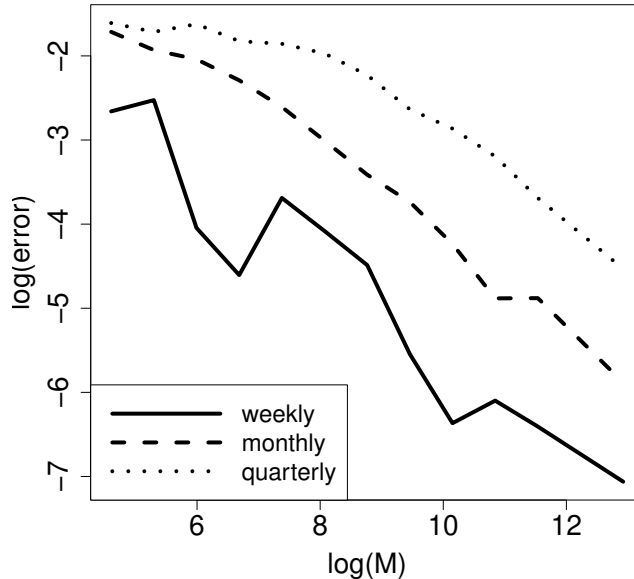


Figure 6: Memorization ratio for three different window sizes for increasing M and N . We choose $N = M$ and $\rho = 0.25$ and consider a correlated geometric Brownian motion in four dimensions as data generation process. The error is the absolute difference of the memorization ratio and its limit.

5.3 Interest rate scenario generation by autoencoders

After illustrating the main principles based on low-dimensional and simple examples, we now consider a purely data-driven setup. We start with interest rate data on a daily basis from 2000-08-01 to 2023-01-31 (more specifically German government rates, taken from the website of the Deutsche Bundesbank¹), containing 5716 data points of dimension 31 (maturities 6M, 1Y, 2Y, ..., 30Y). Since we are interested in yield curve scenarios over the period of a month, we take the observations 1, 21, 41, ..., 5701, leading to 284 independent 1M-differences (one-month differences). Given generated 1M-differences, annual interest rate scenarios for SCR calculations can then be obtained by concatenating twelve 1M-differences.

We use the first 260 difference curves as training data and hold out the remaining 24 difference curves as validation data. As autoencoder setup, we select a fully-connected feed-forward autoencoder with three hidden layers of size 62, 2, and 62 (note that input and output size is 31). Since the number of neurons as well as the number of latent factors (in our setup the dimension of the latent factors Z is two) do not significantly change the results, we have opted for this setup, especially for two latent factors, for simplicity of illustration. Of course, allowing for more latent factors further decreases the reconstruction error.

For the training of the autoencoder, the L-BFGS algorithm has been applied to minimize the mean-absolute-error. All implementations in this section have been carried out in Matlab R2024b, mainly based on the Deep Learning Toolbox. With two latent factors, the final in-sample reconstruction loss is approx. 2 basis points (bp), and out-of-sample 2bp as well, which shows that encoding/decoding can be performed with quite good quality. With four latent factors, it can be further decreased (in-sample and out-of-sample) to 1bp. Figure 7 displays the different type of yield curves the autoencoder can generate when varying the latent factors.

¹https://www.bundesbank.de/dynamic/action/de/statistiken/zeitreihen-datenbanken/zeitreihen-datenbank/759778/759778?listId=www_skms_it03a

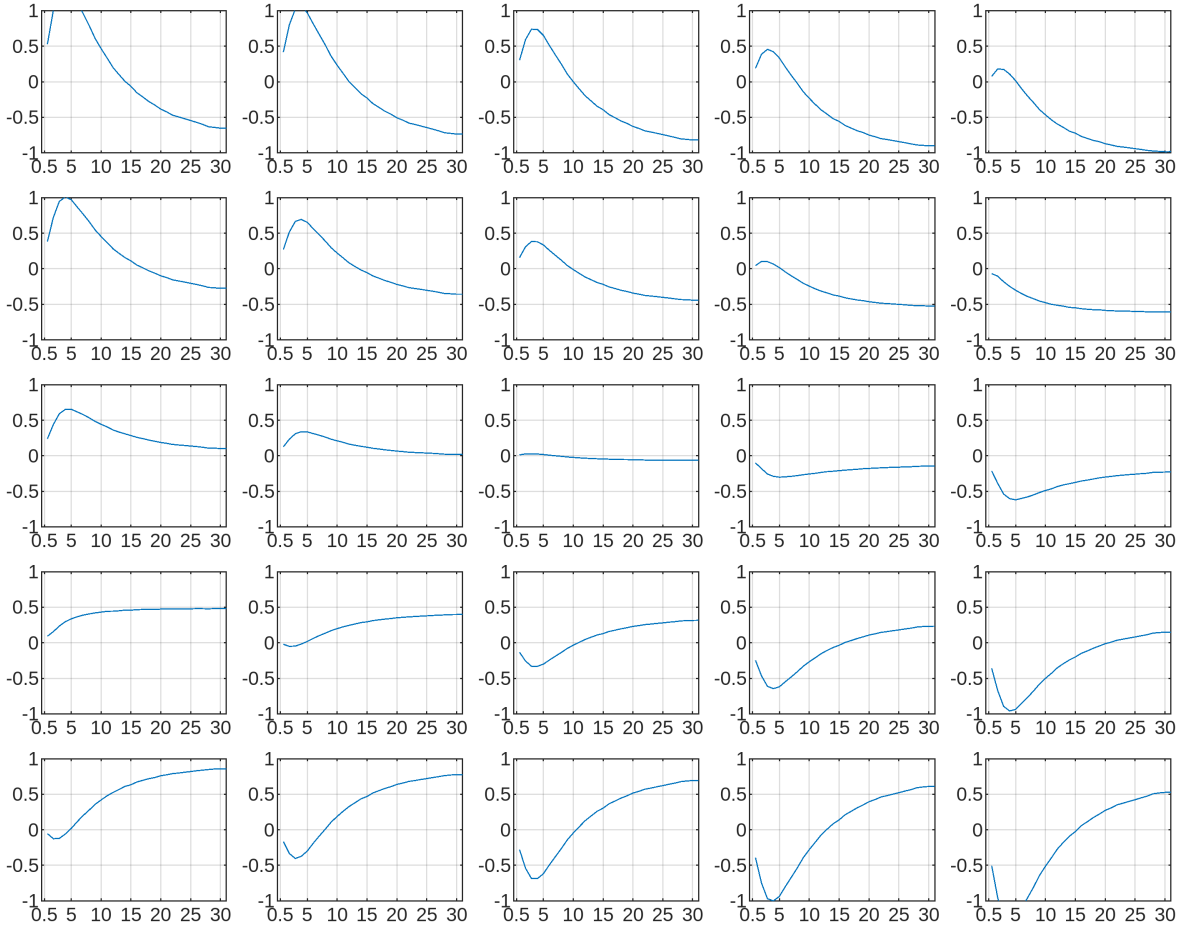


Figure 7: Different types of yield curves (1M-differences) obtained for $Z \in \{-2, -1, 0, 1, 2\}^2$.

In Figure 8, top panel, we have illustrated the 260 latent factors corresponding to the 260 1M-difference curves. In the bottom panel of Figure 8, we have illustrated a random sample for Z according to a 2-dim normal distribution with the same mean and covariance matrix as the latent factors of the training data, whose distribution remains unknown.

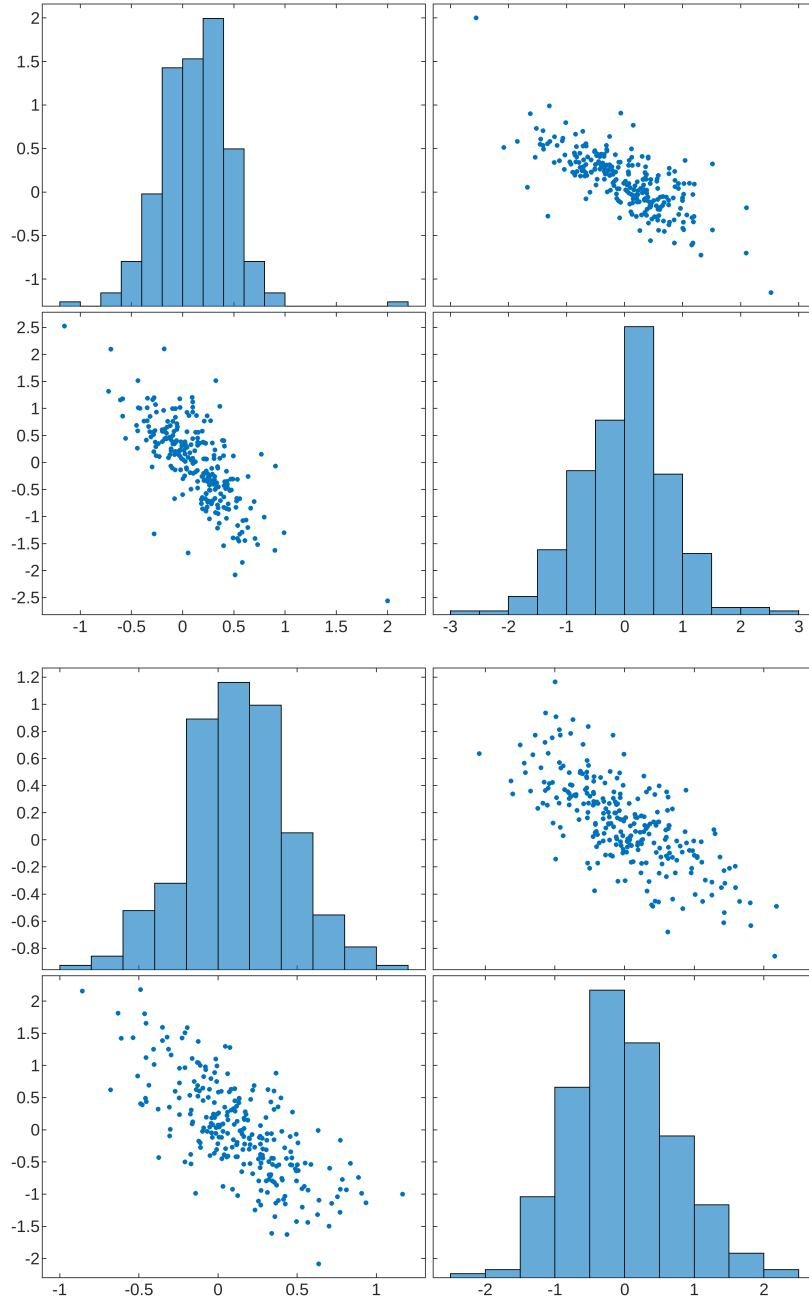


Figure 8: Top panel: marginal distribution and scatter plot of the 260 observations of the latent factors corresponding to the 260 yield curve differences. Bottom panel: marginal distribution and scatter plot of 260 randomly generated scenarios of the latent factors.

Based on the trained autoencoder and its split into an encoder and decoder part, we then generate the following data sets:

- S_1 : In this set, we collect the 260 original 1M-difference curves.
- S_2 : In this set, we collect the 260 encoded and afterwards decoded 1M-difference curves.
- S_3 : This represents the main ML-based generated data, generated by replacing the 260 realizations of the 2-dim latent factor by 260 random realizations of a 2-dim normal distribution with the same mean and covariance matrix as the latent factors.

- S_4 , S_5 and S_6 : New curves are obtained by distorting the elements of S_1 by adding some independent noise with increasing noise level.

Here, the noise for the set S_5 comes from a 31-dim normal distribution with the same mean and the same covariance matrix as the 31-dim reconstruction error of the autoencoder, while the noise for set S_6 is multiplied by 10 (in terms of variance), whereas it is divided by 10 for S_4 .

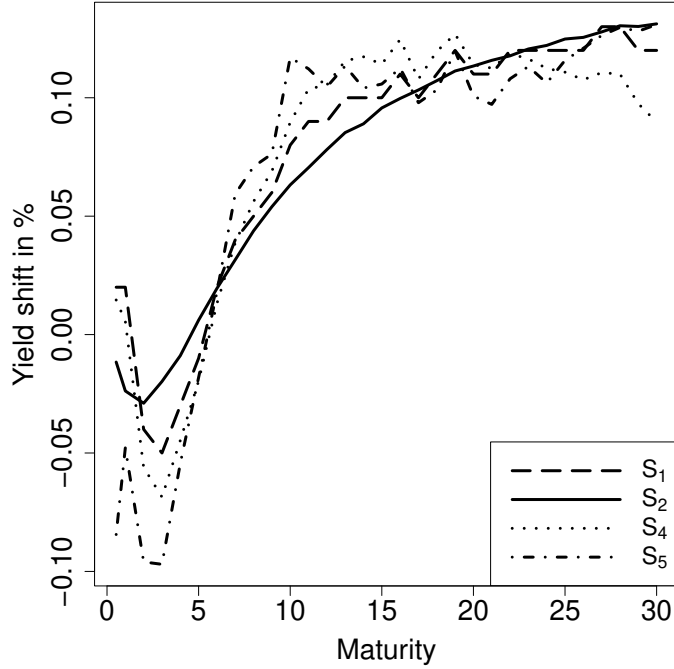


Figure 9: The dashed line represents E_{20} , i.e., the 20-th curve from the training data (S_1), while the solid line represents its encoded-decoded counterpart Y_{20} , i.e., the 20-th element in S_2 . The other two curves are distorted versions of E_{20} , with low noise (S_4) and with a noise level similar to Y_{20} (S_5).

We have illustrated the 1M-difference curves in the sets S_i in Figure 9 by a specific instance (instance no. 20), which represents a typical situation. We can immediately observe that the corresponding curve from S_4 is very close to its original counterpart in S_1 , since the noise is very small. The corresponding curve from S_5 is already further away due to the higher noise, especially at the short end of the yield curve. Note that we did not visualize curves from S_6 because they are too far off. While the encoded-decoded curves from S_2 are also close to the original counterpart (by construction), it can still be observed that curves from S_2 seem to be smoother than all other curves – an often observed feature of autoencoders. Let us recall that the difference between the curves in S_1 and S_2 is solely due to the reconstruction error of the autoencoder, which is on average 1.9bps per tenor, and hence sufficiently small. S_3 has also been left out of the visualization, as this would not make sense, since the randomly generated data is not in a 1-to-1 correspondence to data in the training set.

In Table 4 we have summarized the results of the quantitative comparison of S_2, S_3, \dots, S_6 with S_1 : As expected, S_2 is not too far from S_1 in terms of $T_{NN1,k}$, while the memorization ratio is noticeably higher than its limit $4/9$ under H_0 , which is a clear indicator for memorization. Due to the reconstruction error, the memorization error remains significantly beneath 1, as well as $T_{NN1,k}$ remains significantly above 0. We can further observe ($T_{NN1,k} = 0.15$) that the generated data S_3 is at least as close to the empirical data as is the encoded-decoded data S_2 , while having a much better memorization ratio. Concerning the distorted data, S_5 has a slightly better $T_{NN1,k}$ than S_2 and S_3 , while S_4 is the closest to S_1 , and S_6 is furthest away from S_1 due to its higher level of noise. The memorization ratio decreases with increasing level of noise, which also meets expectations. In summary, we can observe a good performance of the autoencoder-based scenario generation in the column S_3 : we get a similar performance as by disturbing the original data with the same level of noise (i.e. S_5)

– but now, more meaningful (i.e. smoother) yield curves are constructed and the dimension for data generation has been significantly reduced (from 31 to 2).

S_1 compared to	S_2	S_3	S_4	S_5	S_6
$T_{NN1,k}, k = 5$	0.17	0.15	0.09	0.11	0.26
MR, $\rho = 0.80$	0.63	0.51	0.93	0.49	0.09

Table 4: In-sample comparison of the memorization ratio (MR) and the test statistic $T_{NN1,k}$ ($N = M = 260$). Note that under H_0 the memorization ratio (MR) converges to $\frac{\rho}{\rho+1}$, i.e., to $4/9$. We average over 100 simulations and entries in the table come with a standard error of at most ± 0.01 .

To validate our results, we run the following out-of-sample test: Let S_1^* denote the validation set consisting of 24 1M-difference curves. Let S_3^* be ML-based generated data (similar to S_3), generated by replacing the 2-dim latent factor of the autoencoder by 24 random realizations of a corresponding 2-dim normal distribution. The $T_{NN1,k}$ statistic with $k = 5$ between S_1^* and S_3^* is 0.04, i.e., also out-of-sample, we accept the hypothesis that data generated by the autoencoder has the same distribution as the underlying distribution of the empirical data.

Except memorization caused by randomness, it is impossible for the generated set S_3^* to memorize any element of S_1^* since the autoencoder has never seen the validation set S_1^* during training. The memorization ratio with $\rho = 0.8$ between S_1^* and S_3^* is 0.5, which is almost the same as the memorization ratio between S_1 and S_3 . The memorization ratio is only slightly above the theoretical limit of $4/9$ both in-sample and out-of-sample. From this out-of-sample validation, we conclude that the autoencoder does not systematically memorize any training data, since the memorization ratios for in-sample and out-of-sample data are almost equal and close to its theoretical limit.

Regarding the out-of-sample performance of the scenario generator and its adequacy for risk calculations, we need to prove that the generated scenarios S_3 match the out-of-sample distribution of S_1^* sufficiently well: The $T_{NN1,k}$ statistic with $k = 5$ between the out-of-sample data S_1^* and the generated scenarios S_3 is on average 0.04 – indicating that the generated distribution predicts the out-of-sample distribution quite well. A visual inspection of the data in Figure 10 shows that the out-of-sample scenarios are indeed all (perhaps except for two out-of-sample scenarios) covered by the generated scenarios.

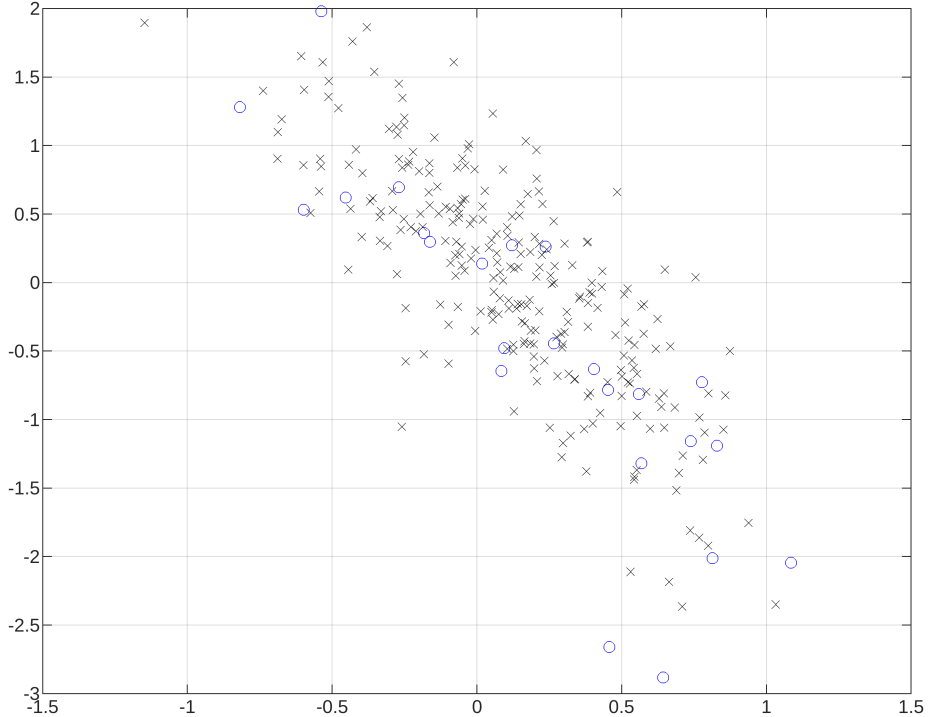


Figure 10: The black 'x' represent data in S_3 , while the blue 'o' represent data in S_1^* . Note that the figure does not show the original 31-dim data, but its encoded 2-dim representation.

Note that 31-dim data cannot be displayed in a 2-dim plot without some projection. We have used coded values, encoded by the autoencoder, but we could have used classical multidimensional scaling for illustration purposes as well. Last but not least, the memorization ratio between S_1^* and S_3 (for $\rho = 0.8$) is 0.88 and thus very close to the theoretical limit of 0.90. As desired, the generated data S_3 almost completely covers the validation data S_1^* . The memorization ratio and the $T_{NN1,k}$ statistic together imply that the generated data does not contain any point of S_1^* (except by chance), but produces a distribution very close to the out-of-sample distribution.

6 Conclusions

When using a ML-based model for regulatory purposes, such as modeling of risks under Solvency 2, additional validation techniques need to be applied to take into account the ML nature of these techniques. For validation purposes, we have provided two specialized measures that can be used to evaluate the performance of the scenario generation: nearest neighbor coincidences (measuring the alignment of the multivariate distributions of the risk factors, see Section 4.1) and a new measure, the memorization ratio (measuring overfitting, see Section 4.2). We show that the memorization ratio converges when the amount of data increases. Numerical experiments on simulated and real market data using several data generation methods (bootstrapping, kernel-smoothing, Monte Carlo and autoencoders) show that the memorization ratio is able to detect the memorization effect.

Acknowledgments and funding

We thank two referees for many helpful comments that significantly improved the paper. Solveig Flaig would like to thank Deutsche Rückversicherung AG for the funding of this research. Opinions, errors and omissions are solely those of the authors and do not represent those of Deutsche Rückversicherung AG or its affiliates.

Disclosure statement.

The authors report there are no competing interests to declare.

Availability of data and materials

All real data analyzed during this study are publicly available. URLs are included in this article.

Code availability

The full code of the experiments presented in this paper is available for review by contacting the corresponding author.

References

- Giovanni Barone Adesi. *Simulating security returns: A filtered historical simulation approach*. Springer, 2014.
- Grigore Albeanu, Manuela Ghica, and Florin Popentiu-Vladicescu. On using bootstrap scenario-generation for multi-period stochastic programming applications. *Int. J. Comput. Commun. Control*, 3:156–161, 2008.
- Hamid Arian, Mehrdad Moghimi, Ehsan Tabatabaei, and Shiva Zamani. Encoded Value-at-Risk: A machine learning approach for portfolio risk measurement. *Mathematics and Computers in Simulation*, 202:500–525, 2022.
- Sanjeev Arora, Rong Ge, Yingyu Liang, Tengyu Ma, and Yi Zhang. Generalization and equilibrium in generative adversarial nets (GANs). In *International conference on machine learning*, pages 224–232. PMLR, 2017.
- Sanjeev Arora, Andrej Risteski, and Yi Zhang. Do GANs learn the distribution? Some theory and empirics. In *International Conference on Learning Representations*, 2018.
- BaFin. Machine learning in risk models: Characteristics and supervisory priorities, 2021. URL <https://www.bundesbank.de/resource/blob/793670/61532e24c3298d8b24d4d15a34f503a8/mL/2021-07-15-ml-konsultationspapier-data.pdf>. [accessed on 2023/10/20].
- Ching-Yuan Bai, Hsuan-Tien Lin, Colin Raffel, and Wendy Chi-wen Kan. On training sample memorization: Lessons from Benchmarking generative modeling with a large-scale competition. In *Proceedings of the 27th ACM SIGKDD Conference on Knowledge Discovery & Data Mining*, pages 2534–2542, 2021.
- Tanya Styblo Beder. VaR: Seductive but dangerous. *Financial Analysts Journal*, 51(5):12–24, 1995.
- Jean-François Bégin. On Complex Economic Scenario Generators: Is Less More? *ASTIN Bulletin: The Journal of the IAA*, 51(3):779–812, 2021.
- Peter J Bickel and Leo Breiman. Sums of functions of nearest neighbor distances, moment bounds, limit theorems and a goodness of fit test. *The Annals of Probability*, pages 185–214, 1983.
- Ali Borji. Pros and cons of GAN evaluation measures. *Computer Vision and Image Understanding*, 179:41–65, 2019.
- Ali Borji. Pros and cons of GAN evaluation measures: New developments. *Computer Vision and Image Understanding*, 215:103329, 2022.
- Robert Buch, Stefanie Grimm, Ralf Korn, and Ivo Richert. Estimating the value-at-risk by Temporal VAE. *Risks*, 11(5):79, 2023.
- Paolo Cadoni. *Internal models and Solvency II*. Risk Books, London, 2014.

- Yize Chen, Pan Li, and Baosen Zhang. Bayesian renewables scenario generation via deep generative networks. In *2018 52nd Annual Conference on Information Sciences and Systems (CISS)*, pages 1–6. IEEE, 2018.
- Rama Cont, Mihai Cucuringu, Renyuan Xu, and Chao Zhang. Tail-GAN: Learning to Simulate Tail Risk Scenarios. *arXiv preprint arXiv:2203.01664*, 2022.
- Omer F Demirel and Thomas R Willemain. Generation of simulation input scenarios using bootstrap methods. *Journal of the Operational Research Society*, 53(1):69–78, 2002.
- Laurent Dupont, Olivier Fliche, and Su Yang. Governance of artificial intelligence in finance, 2020. URL https://acpr.banque-france.fr/sites/default/files/medias/documents/20200612_ai_governance_finance.pdf. [accessed on 2023/10/20].
- Bruno Ebner, Norbert Henze, and Joseph E Yukich. Multivariate goodness-of-fit on flat and curved spaces via nearest neighbor distances. *Journal of Multivariate Analysis*, 165:231–242, 2018.
- European Union. Directive 2009/136/EC of the European parliament and of the council. *Official Journal of the European Union*, 337:11, 2009.
- Lucio Fernandez-Arjona. A neural network model for solvency calculations in life insurance. *Annals of Actuarial Science*, 15(2):259–275, 2021.
- Lucas Benedikt Fiechtner. Risk Management with Generative Adversarial Networks, 2019. URL https://www.researchgate.net/publication/347440941_Risk_Management_with_Generative_Adversarial_Networks. [accessed on 2023/10/20].
- Solveig Flaig and Gero Junike. Scenario generation for market risk models using generative neural networks. *Risks*, 10(11):199, 2022.
- Nadine Gatzert and Michael Martin. Quantifying credit and market risk under Solvency II: Standard approach versus internal model. *Insurance: Mathematics and Economics*, 51(3):649–666, 2012.
- Ian J. Goodfellow, Yoshua Bengio, and Aaron Courville. *Deep Learning*. MIT Press, Cambridge, MA, USA, 2016. <http://www.deeplearningbook.org>.
- Shihao Gu, Bryan Kelly, and Dacheng Xiu. Autoencoder asset pricing models. *Journal of Econometrics*, 222(1):429–450, 2021.
- Darryll Hendricks. Evaluation of value-at-risk models using historical data. *Economic policy review*, 2(1), 1996.
- Norbert Henze. A multivariate two-sample test based on the number of nearest neighbor type coincidences. *The Annals of Statistics*, 16(2):772–783, 1988.
- Carsten Jung, Henrike Mueller, Simone Pedemonte, Simone Plances, and Oliver Thew. Machine learning in UK financial services. *Bank of England and Financial Conduct Authority*, 2019. URL <https://www.bankofengland.co.uk/-/media/boe/files/report/2019/machine-learning-in-uk-financial-services.pdf>. [accessed on 2023/10/20].
- Diederik P. Kingma and Max Welling. *An Introduction to Variational Autoencoders*. 2019.
- Alexei Kondratyev and Christian Schwarz. The market generator. *Available at SSRN 3384948*, 2019.
- David Lopez-Paz and Maxime Oquab. Revisiting classifier two-sample tests. *arXiv preprint arXiv:1610.06545*, 2016.
- Alireza Makhzani, Jonathon Shlens, Navdeep Jaitly, and Ian J. Goodfellow. Adversarial Autoencoders. *CoRR*, abs/1511.05644, 2015. URL <http://arxiv.org/abs/1511.05644>.
- Casey Meehan, Kamalika Chaudhuri, and Sanjoy Dasgupta. A non-parametric test to detect data-copying in generative models. In *International Conference on Artificial Intelligence and Statistics*, 2020.

- Pronoy K Mondal, Munmun Biswas, and Anil K Ghosh. On high dimensional two-sample tests based on nearest neighbors. *Journal of Multivariate Analysis*, 141:168–178, 2015.
- Ulrich A Müller, Roland Bürgi, and Michel M Dacorogna. Bootstrapping the economy—a non-parametric method of generating consistent future scenarios. 2004.
- Vaishnavh Nagarajan, Colin Raffel, and Ian J Goodfellow. Theoretical insights into memorization in GANs. In *Neural Information Processing Systems Workshop*, volume 1, 2018.
- Hao Ni, Lukasz Szpruch, Magnus Wiese, Shujian Liao, and Baoren Xiao. Conditional Sig-Wasserstein GANs for Time Series Generation. *arXiv preprint arXiv:2006.05421*, 2020.
- Hal Pedersen, Mary Pat Campbell, Stephan L Christiansen, Samuel H Cox, Daniel Finn, Ken Griffin, Nigel Hooker, Matthew Lightwood, Stephen M Sonlin, and Chris Suchar. Economic scenario generators: A practical guide. *The Society of Actuaries (July 2016)*, 2016.
- Dietmar Pfeifer and Olena Ragulina. Generating VaR scenarios under Solvency II with product beta distributions. *Risks*, 6(4):122, 2018.
- Matthew Pritsker. The hidden dangers of historical simulation. *Journal of Banking & Finance*, 30(2): 561–582, 2006.
- Adityanarayanan Radhakrishnan, Karren Yang, Mikhail Belkin, and Caroline Uhler. Memorization in overparameterized autoencoders. *arXiv preprint arXiv:1810.10333*, 2018.
- Arne Sandström. *Handbook of solvency for actuaries and risk managers: theory and practice*. CRC press, 2016.
- Matthias Scherer and Gerhard Stahl. The standard formula of Solvency II: a critical discussion. *European Actuarial Journal*, 11:3–20, 2021.
- Mark F Schilling. Multivariate two-sample tests based on nearest neighbors. *Journal of the American Statistical Association*, 81(395):799–806, 1986.
- Shahrok Shedari. *Solvency II. A comparison of the standard model with internal models to calculate the Solvency Capital Requirements (SCR)*. GRIN Verlag, 2016.
- David Tobjörk. Value at Risk Estimation with Generative Adversarial Networks. 2021.
- Gerrit van den Burg and Chris Williams. On memorization in probabilistic deep generative models. *Advances in Neural Information Processing Systems*, 34:27916–27928, 2021.
- Joost van der Burgt. General principles for the use of Artificial Intelligence in the financial sector, 2019. URL <https://www.dnb.nl/media/voffsrc/general-principles-for-the-use-of-artificial-intelligence-in-the-financial-sector.pdf>. [accessed on 2023/10/20].
- EM Varnell. Economic scenario generators and Solvency II. *British Actuarial Journal*, 16(1):121–159, 2011.
- Jiaheng Wei, Yanjun Zhang, Leo Yu Zhang, Ming Ding, Chao Chen, Kok-Leong Ong, Jun Zhang, and Yang Xiang. Memorization in deep learning: A survey. *arXiv preprint arXiv:2406.03880*, 2024.
- Lionel Weiss. Two-sample tests for multivariate distributions. *The Annals of Mathematical Statistics*, 31(1):159–164, 1960.
- Magnus Wiese, Lianjun Bai, Ben Wood, and Hans Buehler. Deep hedging: learning to simulate equity option markets. In *33rd Conference on Neural Information Processing Systems (NeurIPS 2019), Vancouver, Canada*, 2019.
- Magnus Wiese, Robert Knobloch, Ralf Korn, and Peter Kretschmer. Quant GANs: deep generation of financial time series. *Quantitative Finance*, 20(9):1419–1440, 2020.

Qiantong Xu, Gao Huang, Yang Yuan, Chuan Guo, Yu Sun, Felix Wu, and Kilian Weinberger.
 An empirical study on evaluation metrics of generative adversarial networks. *arXiv preprint arXiv:1806.07755*, 2018.

Appendix

A Convergence results

Theorem 2. (Weiss, 1960). Let (Ω, \mathcal{F}, P) be a probability space. Let $E_1, \dots, E_M, G_1, \dots, G_N$ be independent and identically distributed d -variate random variables. Assume E_1 has a piecewise continuous and bounded probability density function f . Let $\mu \in (0, 1]$ and

$$D_m^\mu := \mu \min_{m' \neq m} \|E_m - E_{m'}\|_2, \quad m = 1, \dots, M$$

and let S_m , $m = 1, \dots, M$, be the number of points G_1, \dots, G_N contained in the open sphere $\{x : \|x - E_m\|_2 < D_m^\mu\}$. Then the joint distribution of S_i , S_l is the same as the joint distribution of $S_{i'}$ and $S_{l'}$ for any $i \neq l$ and $i' \neq l'$. It further holds for any $\alpha > 0$ that

$$\lim_{M \rightarrow \infty, \frac{M}{N} = \alpha} P[S_1 = s] = Q(s) := \int_{\mathbb{R}^d} \frac{\mu^{-d}\alpha}{(1 + \mu^{-d}\alpha)^{s+1}} f(x) dx, \quad s \in \mathbb{N}_0 \quad (5)$$

and

$$\lim_{M \rightarrow \infty, \frac{M}{N} = \alpha} P[S_1 = s_1 \cap S_2 = s_2] = Q(s_1)Q(s_2), \quad s_1, s_2 \in \mathbb{N}_0.$$

Proof. Lionel Weiss proved the Theorem for $\mu = \frac{1}{2}$ in Weiss (1960), but his proof works exactly the same for any $\mu \in (0, 1]$. \square

Proof. Proof of Theorem 1: Let $\mu := \rho^{\frac{1}{d}} > 0$. Let Q , D_m^μ , S_m as in Theorem 2. Denote by f the density of E_1 . It holds that

$$Q(0) = \frac{\alpha}{\mu^d + \alpha} \underbrace{\int_{\mathbb{R}^d} f(x) dx}_{=1} = \frac{\alpha}{\rho + \alpha} < \infty.$$

Define R_m as in Equation (3) then $\rho^{\frac{1}{d}} R_m = D_m^\mu$ by the definition of μ . Define

$$Z_m := \mathbf{1}_{[0, \rho^{\frac{1}{d}} R_m)} \left(\min_{n=1, \dots, N} \|G_n - E_m\|_2 \right), \quad m = 1, \dots, M.$$

Then $\Pi_{M,N}^\rho = \frac{1}{M} \sum_{m=1}^M Z_m$ and

$$\begin{aligned} \mathbf{E}[Z_m] &= P \left[\min_{n=1, \dots, N} \|G_n - E_m\|_2 < \rho^{\frac{1}{d}} R_m \right] \\ &= 1 - P \left[\forall n : \|G_n - E_m\|_2 \geq \rho^{\frac{1}{d}} R_m \right] \\ &= 1 - P[S_m = 0] \\ &= 1 - P[S_1 = 0]. \end{aligned}$$

It follows by Theorem 2 that

$$\lim_{M \rightarrow \infty, \frac{M}{N} = \alpha} \mathbf{E}[Z_m] = 1 - Q(0) = \frac{\rho}{\rho + \alpha}. \quad (6)$$

As $Z_m^2 = Z_m$, it follows that

$$\lim_{M \rightarrow \infty, \frac{M}{N} = \alpha} \text{Var}(Z_m) = 1 - Q(0) - (1 - Q(0))^2 = \frac{\rho\alpha}{(\rho + \alpha)^2} < \infty, \quad m = 1, 2, \dots$$

Let $i \neq l$. Then

$$\begin{aligned}
\text{Cov}(Z_i, Z_l) &= \mathbf{E}[Z_i Z_l] - \mathbf{E}[Z_i] \mathbf{E}[Z_l] \\
&= P \left(\min_{n=1, \dots, N} \|G_n - E_i\|_2 < \rho^{\frac{1}{d}} R_i \cap \min_{n=1, \dots, N} \|G_n - E_l\|_2 < \rho^{\frac{1}{d}} R_l \right) - (\mathbf{E}[Z_1])^2 \\
&= 1 - P[S_i = 0 \cup S_l = 0] - (\mathbf{E}[Z_1])^2 \\
&= 1 - P[S_1 = 0 \cup S_2 = 0] - (\mathbf{E}[Z_1])^2 \\
&= 1 - P[S_1 = 0] - P[S_2 = 0] + P[S_1 = 0 \cap S_2 = 0] - (\mathbf{E}[Z_1])^2.
\end{aligned}$$

Therefore we have that

$$\lim_{M \rightarrow \infty, \frac{M}{N} = \alpha} \text{Cov}(Z_i, Z_l) = 1 - Q(0) - Q(0) + Q^2(0) - (1 - Q(0))^2 = 0.$$

By Bienaymé's identity it follows that

$$\begin{aligned}
\mathbf{E} \left[\left| \Pi_{M,N}^\rho - \mathbf{E}[Z_1] \right|^2 \right] &= \text{Var} \left(\frac{1}{M} \sum_{i=1}^M Z_i \right) \\
&= \frac{1}{M^2} \left(\sum_{i=1}^M \text{Var}(Z_i) + \sum_{i \neq l} \text{Cov}(Z_i, Z_l) \right) \\
&= \frac{1}{M^2} (M \text{Var}(Z_1) + (M^2 - M) \text{Cov}(Z_1, Z_2)).
\end{aligned}$$

Thus,

$$\lim_{M \rightarrow \infty, \frac{M}{N} = \alpha} \mathbf{E} \left[\left| \Pi_{M,N}^\rho - \mathbf{E}[Z_1] \right|^2 \right] = 0. \quad (7)$$

Further, by the Minkowski inequality, it holds that

$$\sqrt{\mathbf{E} \left[\left| \Pi_{M,N}^\rho - \frac{\rho}{\rho + \alpha} \right|^2 \right]} \leq \sqrt{\mathbf{E} \left[\left| \Pi_{M,N}^\rho - \mathbf{E}[Z_1] \right|^2 \right]} + \sqrt{\mathbf{E} \left[\left| \mathbf{E}[Z_1] - \frac{\rho}{\rho + \alpha} \right|^2 \right]}.$$

Apply Equation (6) and Equation (7) to conclude. \square

B Technical details: dependent data

Let $M, N \in \mathbb{N}$. Assume a business year has 252 days and a month consists of 21 business days. Let $\delta = \frac{1}{252}$. Let W^1, \dots, W^d be independent standard Brownian motions. Let $\Sigma \in \mathbb{R}^{d \times d}$ be symmetric positive definite. Let A such that $AA^\top = \Sigma$. Define

$$S_t^i = S_0^i \exp \left[\left(r - \frac{1}{2} \sum_{h=1}^d A_{ih}^2 \right) t + \sum_{h=1}^d A_{ih} W_t^h \right], \quad i = 1, \dots, d.$$

We set $S_0^i = 1$, $r = 0$, $\Sigma_{ii} = \sigma^2$, $\Sigma_{ij} = \sigma^2 \gamma$ with $\sigma = 0.2$ and correlation $\gamma = 0.7$. We consider a d -dimensional time series of daily prices of length $M + N + 2w$, i.e.,

$$S_0^i, \dots, S_{\delta(M+N+2w-1)}^i, \quad i = 1, \dots, d.$$

Based on this time series of $M + N + 2w$ daily prices, we will construct two samples of length M and N of log-returns over a time horizon of w days: Let

$$E_m^i = \log \left(\frac{S_{\delta(m-1+w)}^i}{S_{\delta(m-1)}^i} \right), \quad i = 1, \dots, d, \quad m = 1, \dots, M$$

and

$$G_n^i = \log \left(\frac{S_{\delta(M+w+n-1+w)}^i}{S_{\delta(M+w+n-1)}^i} \right), \quad i = 1, \dots, d, \quad n = 1, \dots, N.$$

If $w = 1$ then E_m^i correspond to daily log-returns and E_m^i and $E_{m'}^i$ for $m \neq m'$ are independent. If $w = 21$ then E_m^i corresponds to monthly log-returns. The two groups E_1, \dots, E_M and G_1, \dots, G_N are independent. However, in the time-dimension, the points inside a group are not necessarily independent: Let $m > m'$. If $m \geq w + m'$ then E_m^i and $E_{m'}^i$ are independent since the Brownian motions have independent increments, otherwise, they are correlated. A similar statement holds for G_n^i and $G_{n'}^i$.

C R Code

The following R code implements the statistic $\Pi_{M,N}^{\rho}$ in the function `memorizationRatio()` and the statistic $T_{NN1,k}$ in the function `TNN1k()`. Feel free to replace the for-loops with the function `mclapply` from the *parallel* package to parallelize the code.

```

#Input: matrix D and row number i.
#Returns: vector of sorted distances of vector D[i, ] to rows of matrix D[-i, ].
disIn = function(D, i){
  return(sqrt(rowSums((matrix(D[i, ], nrow = (nrow(D)-1), ncol = ncol(D), byrow = T) - D[-i, ])^2)))
}

#Input: matrix D and vector x with length equal to number of columns of D.
#Returns: vector of length nrow(D) of sorted distances of x to rows of D.
disOut = function(x, D){
  return(sqrt(rowSums((matrix(x, nrow = nrow(D), ncol = ncol(D), byrow = T) - D)^2)))
}

#Input: vectors x and y and integer k in {1,...,length(x)}
#Returns: the number of elements of x which are in the first k entries of the contacted and sorted vector c(x, y).
numberSameNearestNeighbor = function(x, y, k){
  tmp = matrix(c(x, y, rep(1, length(x)), rep(0, length(y))), ncol = 2)
  return(sum(tmp[order(tmp[, 1]), ][1:k, 2]))
}

#Input: M x d matrix of empirical data, N x d matrix of generated data, rho in (0,1]
#Returns: memorization ratio
memorizationRatio = function(E, G, rho){
  d = ncol(E)
  M = nrow(E)
  N = nrow(G)
  MR = 0
  for(m in 1:M){
    myDisOut = disOut(E[m,], G) #Distance of Em to generated data points
    myDisIn = disIn(E, m) #Distance of Em to other empirical data points
    if(min(myDisOut) < (min(myDisIn) * rho^(1 / d))){
      MR = MR + 1
    }
  }
  return(MR / M)
}

#Input: M x d matrix of empirical data, N x d matrix of generated data, k in {1, 2,...}
#Returns: the statistic TNN1k
TNN1k = function(E, G, k){
  d = ncol(E)
  M = nrow(E)
  N = nrow(G)
  TEk = 0
  TGk = 0
  for(m in 1:M){
    myDisOut = disOut(E[m,], G) #Distance of Em to generated data points
    myDisIn = disIn(E, m) #Distance of Em to other empirical data points
    TEk = TEk + numberSameNearestNeighbor(myDisIn, myDisOut, k)
  }
}

```



```

}
for(n in 1:N){
  myDisOut = disOut(G[n,], E) #Distance of Gn to empirical data points
  myDisIn = disIn(G, n) #Distance of Gn to other generated data points
  TGk = TGk + numberSameNearestNeighbor(myDisIn, myDisOut, k)
}
TEk = TEk / (M * k)
TGk = TGk / (N * k)
return((M * abs(TEk - (M - 1) / (M + N - 1)) + N * abs(TGk - (N - 1) / (M + N - 1))) / (N + M))
}

```

D Data

Year	Log-returns	S&P 500 Jan.	S&P 500 Dec.	Training/ Testing
1997	0.2751	737.01	970.43	Training
1998	0.2317	975	1229.23	Training
1999	0.1793	1228.1	1469.25	Training
2000	-0.0973	1455.22	1320.28	Training
2001	-0.1113	1283.27	1148.08	Training
2002	-0.2719	1154.67	879.82	Training
2003	0.1994	909.03	1109.64	Training
2004	0.0892	1108.48	1211.92	Training
2005	0.0377	1202.08	1248.29	Training
2006	0.1114	1268.8	1418.3	Training
2007	0.0347	1418.3	1468.36	Training
2008	-0.4714	1447.16	903.25	Training
2009	0.1796	931.8	1115.1	Training
2010	0.1044	1132.99	1257.64	Training
2011	-0.0113	1271.89	1257.6	Training
2012	0.1104	1277.06	1426.19	Testing
2013	0.2342	1462.42	1848.36	Testing
2014	0.1168	1831.98	2058.9	Testing
2015	-0.0070	2058.2	2043.94	Testing
2016	0.1065	2012.66	2238.83	Testing
2017	0.1690	2257.83	2673.61	Testing
2018	-0.0727	2695.81	2506.85	Testing
2019	0.2524	2510.03	3230.78	Testing
2020	0.1423	3257.85	3756.07	Testing
2021	0.2530	3700.65	4766.18	Testing
2022	-0.2226	4796.56	3839.5	Testing
2023	0.2210	3824.14	4769.83	Testing

Table 5: S&P 500, yearly log-returns between beginning of January and end of December for the years 1997 till 2023.